Vol 18 No 9, September 2009
1674-1056/2009/18(09)/3952-08

Chinese Physics B

© 2009 Chin. Phys. Soc.
and IOP Publishing Ltd

Experimental determination of interfacial energies for Ag_2Al solid solution in the $CuAl_2$–Ag_2Al system*

Ocak Y[a)b)], Akbulut S[b)], Keşlioğlu K[a)],
Maraşlı N[a)†], Çadırlı E[c)], and Kaya H[d)]

[a)] *Department of Physics, Faculty of Arts and Sciences, Erciyes University, Kayseri 38039, Turkey*
[b)] *Department of Physics, Institute of Science and Technology, Erciyes University, Kayseri 38039, Turkey*
[c)] *Department of Physics, Faculty of Arts and Sciences, Niğde University, Niğde, Turkey*
[d)] *Department of Science Education, Education Faculty, Erciyes University, Kayseri 38039, Turkey*

(Received 28 January 2009; revised manuscript received 27 February 2009)

The equilibrated grain boundary groove shapes of solid solution Ag_2Al in equilibrium with an Al–Cu–Ag liquid were observed from a quenched sample with a radial heat flow apparatus. The Gibbs–Thomson coefficient, solid–liquid interfacial energy and grain boundary energy of the solid solution Ag_2Al have been determined from the observed grain boundary groove shapes. The thermal conductivity of the solid phase and the thermal conductivity ratio of the liquid phase to solid phase for Ag_2Al–28.3 at the $\%CuAl_2$ alloy at the melting temperature have also been measured with a radial heat flow apparatus and Bridgman type growth apparatus, separately.

Keywords: solid–liquid interfaces, metals and alloys, surface energy, thermal conductivity
PACC: 6810C, 6840, 7430E, 7520E

1. Introduction

The solid–liquid interfacial energy, σ_{SL}, is recognized as playing a key role in a wide range of metallurgical and materials phenomena from wetting[1] and sintering through phase transformations and coarsening.[2] Thus, a quantitative knowledge of σ_{SL} values is necessary. However, the determination of σ_{SL} is difficult. Since 1985, a technique for the quantification of solid–liquid interfacial free energy from the grain boundary groove shape has been established. This technique is based on the direct application of the Gibbs–Thomson equation and can be used to measure σ_{SL} for multi-component systems as well as pure materials, for opaque materials as well as transparent materials, for any observed grain boundary groove shape and for any value of the thermal conductivity ratio of the equilibrated liquid phase to solid phase, $R = K_L/K_S$. Measurements of the solid–liquid interface energies were made in pure materials and alloys.[3–36]

More recently, the phase diagram of the aluminum (Al)–silver (Ag)–copper (Cu) system has been evaluated[37] and a part of the phase diagram is shown in Fig.1. Some thermophysical properties such as solid–liquid interfacial energy, Gibbs–Thomson coefficient, grain boundary energy and thermal conductivities of the solid and liquid phases have not been well known. These thermophysical properties could be of use to people doing comparisons between experimentally observed solidification morphology and predictions from theoretical models. Thus the aims of the present work were to observe the grain boundary groove shapes of solid solution Ag_2Al in equilibrium with an Al–Cu–Ag liquid and to determine the Gibbs–Thomson coefficient, solid–liquid interfacial energy and grain boundary energy for the solid solution Ag_2Al from the observed grain boundary groove shapes.

2. Materials and methods

2.1. Sample production

The phase diagram of the $CuAl_2$–Ag_2Al system has been evaluated[37] as shown in Fig.1. From the phase diagram, the composition of the alloy was chosen to be Ag_2Al–28.3at$\%CuAl_2$ to grow a single phase

*This research was financially supported by the Scientific and Technical Research Council of Turkey (TÜBİTAK (Grant No 105T481).
†Corresponding author. E-mail: marasli@erciyes.edu.tr

solid solution Ag_2Al (Ag_2Al–28.3at%$CuAl_2$) in the cast state. An Ag_2Al–28.3at%$CuAl_2$ alloy was prepared in a vacuum furnace by using 99.9% pure aluminum, 99.99% pure silver and 99.9% pure copper. After stirring, the molten alloy was poured into a graphite crucible held in a specially constructed casting furnace at approximately 50 K above the melting point of the alloy. The molten metal was then directionally solidified from bottom to top to ensure that the crucible was completely full.

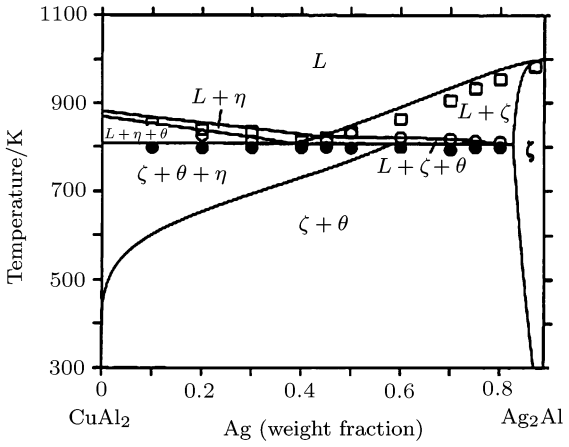


Fig.1. The phase diagram of Cu_2Al–Ag_2Al.[37]

In order to observe the equilibrated grain boundary groove shapes in opaque materials, Gündüz and Hunt[15,16] designed a radial heat flow apparatus. Maraşli and Hunt[17] improved the experimental apparatus for higher temperatures. The details of the apparatus and experimental procedures are given in Refs.[15]–[17]. In the present work, a similar apparatus was used to observe the grain boundary groove shapes in the Al–Cu–Ag ternary alloy.

The sample was heated from the centre by a single heating wire and the outside of the sample was kept constant to an accuracy of ±0.01 K at 293 K (20 °C) using a Poly Science digital 9102 model heating/refrigerating circulating bath to get a constant radial temperature gradient on the sample. A thin liquid layer was melted around the central heating wire and annealed for a sufficient period in a constant radial temperature gradient. The temperature on the sample was controlled to an accuracy of ±0.01 K with a Eurotherm 2604 type controller. The annealing time for the Ag_2Al–28.3at%$CuAl_2$ specimen was 4 days. During the annealing period, the temperature in the solid phase and the vertical temperature variations on the specimen were continuously recorded by the stationary thermocouples and a movable thermocouple, respectively, by using a data logger via a computer. The input power was also recorded periodically. The temperature in the sample was stable to about ±0.025 K for hours and ±0.05 K for up to 4 days. At the end of the annealing time the specimen was rapidly quenched by turning off the input power which is sufficient to get a well-defined solid–liquid interface, because the liquid layer around the central heating wire was very thin (typically less than 0.5–1 mm).

2.2. Measurements of the coordinates of equilibrated grain boundary groove shapes

The quenched sample was cut transversely into lengths typically 25 mm and the transverse sections were ground flat with 180 grit SiC paper. Grinding and polishing were then carried out by following the standard route. After polishing, the samples were etched with a 14 ml sulfuric acid, 2.5 gr (1 gr=0.064799 g) molybdic acid in 50 ml water for 10 seconds.

The equilibrated grain boundary groove shapes were then photographed with an Olympus DP12 type CCD digital camera placed in conjunction with an Olympus BX51 type light optical microscope. A graticule ($200 \times 0.01 = 2$ mm) was also photographed using the same objective. The photographs of the equilibrated grain boundary groove shapes and the graticule were superimposed on one another using Adobe PhotoShop 8.0 version software so that an ccurate measurement of the groove coordinate points on the groove shapes could be made.

2.3. Geometrical correction for the groove coordinates

The coordinates of the cusp (x, y) should be measured using the coordinates (x, y, z) where the x axis is parallel to the solid–liquid interface, the y axis is normal to the solid–liquid interface and the z axis lies at the base of the grain boundary groove. The coordinates of the cusp (x', y') from the metallographic section must be transformed to the (x, y) coordinates. Maraşlı and Hunt[17] devised a geometrical method to make appropriate corrections to the groove shapes and the details of the geometrical method are given in Ref.[17].

The coordinates of equilibrated grain boundary groove shapes were measured with an optical microscope to an accuracy of ±10 μm by following the Maraşlı and Hunt geometrical method so that appropriate corrections to the shape of the grooves could be deduced.[17]

2.4. Measurements of the thermal conductivity of the solid and liquid phases

The thermal conductivity ratio of the equilibrated eutectic liquid phase ($CuAl_2$–23.6at%Ag_2Al) to the solid solution Ag_2Al phase (Ag_2Al–28.3at%$CuAl_2$), $R = K_{L(\text{eutecticliquid})}/K_{S(Ag_2Al)}$ must be known or measured to evaluate the Gibbs–Thomson coefficients with the present numerical method. The radial heat flow method is an ideal technique for measuring the thermal conductivity of the solid phases. The thermal conductivity of the solid solution Ag_2Al phase is also needed to evaluate the temperature gradient on the solid phases. Under the steady-state condition, the temperature gradients in the cylindrical specimen is given by Fourier's law

$$\frac{dT}{dr} = -\frac{Q}{AK_S}, \tag{1}$$

where Q is the total input power from the centre of the specimen, A is the surface area of the specimen and K_S is the thermal conductivity of the solid phase. Integration of the Eq.(1) gives

$$K_S = a_0 \frac{Q}{T_1 - T_2}, \tag{2}$$

where $a_0 = \ln(r_2/r_1)2\pi\ell$ is an experimental constant, r_1 and r_2 ($r_2 > r_1$) are fixed distances from the centre axis of the specimen, ℓ is the length of the heating wire which is constant, and T_1 and T_2 are the temperatures at the fixed positions, r_1 and r_2. Equation (2) could be used to obtain the thermal conductivity of the solid phase by measuring the difference in temperature between two fixed points for a given power level provided that the vertical temperature variations is minimum or zero.

The thermal conductivity of the solid solution Ag_2Al phase (Ag_2Al–28.3at%$CuAl_2$) was measured in the radial heat flow apparatus. The sample production was made as mentioned in Section 2.1. The specimen was heated from the centre using a single heating wire (140–190 mm in length and 2.5 mm in diameter, Kanthal A-1) in steps of 50 K up to 10 K below the melting temperature of the material and the outside of the specimen was cooled to get the radial temperature gradient. To get the reliable value of thermal conductivity in the thermal conductivity measurement, larger radial temperature gradient is desired. For this purpose, the gap between the cooling jacket and the specimen was filled with free running sand or graphite dust and the outside of the specimen was kept at 293 K using a heating/refrigerating circulating bath. The length of the central heating wire was chosen to be 10 mm longer than the length of the specimen to make isotherms parallel to the vertical axis.

The specimen was kept at a steady state condition for at least two hours at a setting temperature. In a steady state, the total input power and the stationary thermocouples temperatures were recorded with a Hewlett Packard 34401 type multimeter and a Pico TC-08 data-logger. After all desired power settings and temperature measurements had been completed during the heating procedure, the cooling procedure was started in same steps down to room temperature. The experimental value of a_0 for the solid solution Ag_2Al phase (Ag_2Al–28.3at%$CuAl_2$) was 1.505 m^{-1} in the present work.

The thermal conductivity of the solid solution Ag_2Al phase versus temperature is shown in Fig.2. The value of K_S for the solid solution Ag_2Al phase (Ag_2Al–28.3at%$CuAl_2$) at the eutectic melting temperature was obtained to be 46.0 W/(K·m), by extrapolating to the eutectic temperature as shown in Fig.2. The values of thermal conductivities used in the determination of the Gibbs–Tomson coeffient are given in Table 1.

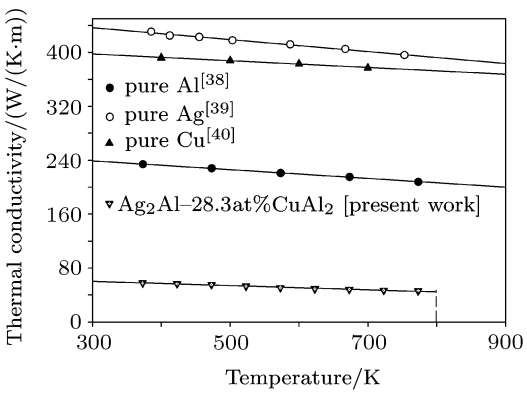


Fig.2. Thermal conductivity of the Ag_2Al–28.3at%$CuAl_2$ alloy solid phase versus temperature.

Table 1. Thermal conductivity of specific solid and liquid phases in the Al–Cu–Ag ternary alloy at their melting temperature.

alloy	phases	melting temperature/K	K/(W/K·m)	$R = K_L/K_S$
Al–Cu–Ag	liquid (Al–16.57at%Ag–11.87at%Cu)	775.09	55.4 [36]	1.42
	solid (Ag–38.60at%Al–2.93at%Cu)		38.9 [36]	
	liquid ($CuAl_2$–23.6at%Ag_2Al)	799.35	42.0	0.91
	solid Ag_2Al (Ag_2Al–28.3at%$CuAl_2$)		46.0	

It is not possible to measure the thermal conductivity of the liquid phase with the radial heat flow apparatus since a thick liquid layer (10 mm) is required. A layer of this size would certainly have led to convection. If the thermal conductivity ratio of the liquid phase to the solid phase is known and the thermal conductivity of the solid phase is measured at the melting temperature, the thermal conductivity of the liquid phase can then be evaluated. The thermal conductivity ratio can be obtained during directional growth with a Bridgman type growth apparatus. The detail of the experimental procedure was given in Refs.[17]–[24].

The thermal conductivity ratio of the eutectic liquid ($CuAl_2$–23.6at%Ag_2Al) to the solid solution Ag_2Al phase (Ag_2Al–28.3at%$CuAl_2$) $R = K_{L(\text{eutectic})}/K_{S(Ag_2Al)}$ was measured to be 0.91 as shown in Fig.3. The values of K_L and K_S used in the determination of Gibbs–Thomson coefficient are also given in Table 1.

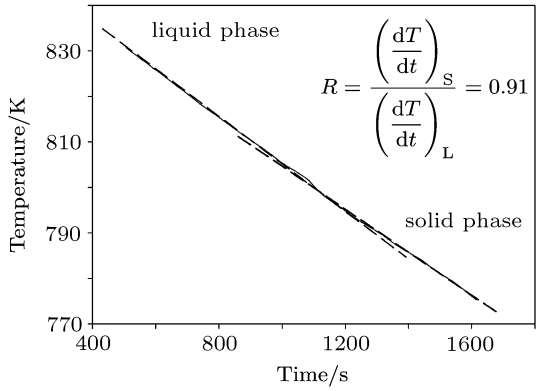


Fig.3. Cooling rate of Ag_2Al–28.3at%$CuAl_2$ alloy.

A comparison of the values of K_S and K_L for the solid solution Ag_2Al and the $CuAl_2$–23.6at%Ag_2Al liquid obtained in the present work with the values of K_S and K_L for the solid solution Ag_2Al and $CuAl_2$–23.6at%Ag_2Al liquid obtained in the previous work is given in Table 1. As can be seen from Table 1, the value of K_S for the solid solution Ag_2Al obtained in the present work is about 15% bigger than the value of K_S for the same solid phase obtained by Bulla *et al*[36] but the value of $R = K_{L(\text{eutectic})}/K_{S(Ag_2Al\text{solution})}$ obtained by Bulla *et al*[36] is about 50% bigger than the value of $R = K_{L(\text{eutectic})}/K_{S(Ag_2Al\text{solution})}$ obtained in present work.

2.5. Measurement of temperature gradient in the solid phase

The cylindrical sample was heated from the centre by a thin heating wire and a thin liquid layer was melted around the central heating wire. At the steady-state the temperature gradient at radius r is given by

$$G_s = \frac{dT}{dr} = -\frac{Q}{2\pi r \ell K_S}, \tag{3}$$

where Q is the input power, ℓ is the length of the heating wire, r is the distance of the solid–liquid interface to the centre of the sample and K_S is the thermal conductivity of the solid phase.

The average temperature gradient of the solid phase must be determined for each grain boundary groove shape. This was done by measuring the input power, the length of the heating wire and the position of the solid–liquid interface and the value of K_S for the solid solution Ag_2Al phase at the eutectic melting point. By using these measured values in Eq.(3) the temperature gradient can be determined for each grain boundary groove shape.

3. Results and discussions

3.1. Determination of the Gibbs–Thomson coefficient

If the thermal conductivity ratio of the equilibrated liquid phase to solid phase, the coordinates of the grain boundary groove shape and the temperature gradient of the solid phase are known, the Gibbs–Thomson coefficient (Γ) can be obtained using the

numerical method described in detail in Ref.[15]. The experimental error in the determination of the Gibbs–Thomson coefficient is the sum of experimental errors in the measurement of the temperature gradient, thermal conductivity and groove coordinates. Thus the total error in the determination of the Gibbs–Thomson coefficient is about 7%.[17]

The Gibbs–Thomson coefficients for the solid solution Ag_2Al in equilibrium with the eutectic Al–Cu–Ag liquid were determined with the present numerical model by using ten equilibrated grain boundary groove shapes. Typical grain boundary groove shapes for the solid Ag_2Al solution in equilibrium with the eutectic liquid ($CuAl_2$–23.6at%Ag_2Al) are shown in Fig.4.

As can be seen from Fig.4, a very thin $CuAl_2$ (Al–32.31at%Cu–0.04at%Ag) layer which is smaller than 1 μm formed in front of the solid solution Ag_2Al phase (Ag_2Al–28.3at%$CuAl_2$) and this allows a well defined solid–liquid interface to be observed during the quench. Also the phases, grains and interfaces of the system are very clear. The values of Γ for the solid solution Ag_2Al are given in Table 2. The average value of Γ from Table 2 is $(3.5\pm0.3)\times10^{-8}$ Km for the solid solution Ag_2Al in equilibrium with Al–Cu–Ag liquid.

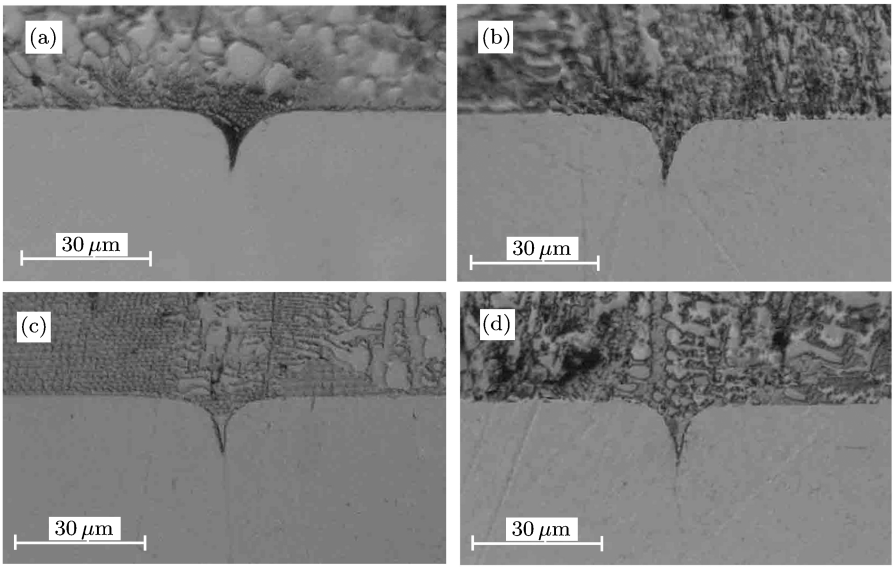


Fig.4. Typical grain boundary groove shapes for the solid solution Ag_2Al in equilibrium with $CuAl_2$–23.6 at%Ag_2Al eutectic liquid.

Table 2. Gibbs–Thomson coefficients for the solid Ag_2Al solution in equilibrium with the Al-Cu-Ag ($CuAl_2$–23.6at%Ag_2Al) eutectic liquid. The subscripts LHS and RHS refer to the left-hand side and the right-hand side of the groove, respectively.

grove No	$G_K \times 10^2$ /(K/m)	α	β	Gibbs–Thomson coefficient	
				$\Gamma_{LHS} \times 10^{-8}$/(K·m)	$\Gamma_{RHS} \times 10^{-8}$/(K·m)
a	18.3	23.5	17.8	3.5	3.7
b	18.5	15.0	15.2	3.6	3.3
c	20.0	24.1	28.2	3.7	3.6
d	16.9	11.2	10.9	3.8	3.7
e	19.8	7.3	8.9	3.7	3.6
f	13.2	6.3	11.2	3.6	3.8
g	18.5	5.7	12.0	3.3	3.4
h	18.3	17.6	16.1	3.7	3.7
i	17.6	18.2	16.5	3.3	3.4
j	19.0	10.9	9.2	3.2	3.4
				$\bar{\Gamma} = (3.5 \pm 0.3) \times 10^{-8}$ K·m	

3.2. Determination of entropy of fusion per unit volume

In order to determine the solid–liquid interfacial energy it is also necessary to know the entropy of fusion per unit volume, ΔS_f for the solid phase. The entropy change per unit volume for an alloy is given by[15]

$$\Delta S_f = \frac{(1-C_S)(S_A^L - S_A^S) + C_S(S_B^L - S_B^S)}{V_S}, \quad (4)$$

where S_A^L, S_A^S, S_B^L and S_B^S are partial molar entropies for A and B materials, respectively and C_S is the composition of the solid phase. Since the entropy terms are generally not available, for convenience, the undercooling at constant composition may be related to the change in composition at constant temperature. For a solid sphere of radius r[41]

$$\Delta C_r = \frac{2\sigma_{SL} V_S (1-C_L) C_L}{rRT_M(C_S - C_L)}, \quad (5)$$

where R is the gas constant, T_M is the melting temperature and V_S is the molar volume of the solid phase. For small changes

$$\Delta T_r = m_L \Delta C_r = \frac{2m_L \sigma_{SL} V_S (1-C_L) C_L}{rRT_M(C_S - C_L)}, \quad (6)$$

where m_L is the slope of liquidus. For spherical solids, the curvature undercooling is

$$\Delta T_r = \frac{2\sigma_{SL}}{r\Delta S_f}. \quad (7)$$

From Eqs.(6) and (7), the entropy change for an alloy is written as

$$\Delta S_f = \frac{RT_M}{m_L V_S} \frac{C_S - C_L}{(1-C_L)\,C_L}. \quad (8)$$

The molar volume, V_S is expressed as

$$V_S = V_C N_A \frac{1}{n}, \quad (9)$$

where V_C is the volume of the unit cell, N_A is the Avogadro's number and n is the number of molecules per unit cell. The values of the relevant constant used in the determination of entropy change per unit volume were obtained from Fig.1 and they are given in Table 3. The error in the determination of entropy change of fusion per unit volume is estimated to be about 5%.[42]

Table 3. Some thermophysical properties of the solid solution Ag_2Al in the Al–Cu–Ag alloy.

system	Al–Cu–Ag
composition of solid phase C_S	solid solution Ag_2Al (Ag_2Al–28.3at%$CuAl_2$)[37]
composition of liquid phase C_L	eutectic liquid ($CuAl_2$–23.6at%Ag_2Al)[37]
$f(C)$[a]	2.67
melting temperature T_m/K	799.35
molar volume of solid solution Ag_2Al, $V_{Ag_2Al} \times 10^{-6}/m^3$	10.1[43]
liquidus slope of solid solution Ag_2Al, m_L/(K/at%)	426.02
entropy change of fusion for solid Ag_2Al, $\Delta S_f/(J/K{\cdot}m^3)$	4.12×10^6

[a] $f(C) = \dfrac{C_S - C_L}{(1-C_L)\,C_L}$

3.3. Evaluation of solid–liquid interfacial energy

The solid–liquid interfacial energy, σ_{SL} can be obtained from the thermodynamic definition of the Gibbs–Thomson equation for isotropic interfacial energy[15] and it is expressed as

$$\Gamma = \frac{\sigma_{SL}}{\Delta S_f}. \quad (10)$$

If the values of Γ and ΔS_f are known the value of solid–liquid interfacial energy, σ_{SL} can be evaluated from Eq.(10). The solid–liquid interfacial energy of the solid solution Ag_2Al (Ag_2Al–28.3at%$CuAl_2$) in equilibrium with Al–Cu–Ag eutectic liquid ($CuAl_2$–23.6at%Ag_2Al) was evaluated to be $(145.9 \pm 17.5) \times 10^{-3} J{\cdot}m^{-2}$ using the values of Γ and ΔS_f. The experimental error in the determination of solid–liquid interfacial energy is the sum of experimental errors of the

Gibbs–Thomson coefficient and the entropy change of fusion per unit volume. Thus, the total experimental error of the solid–liquid interfacial energy evaluation in the present work is about 12%.

3.4. Grain boundary energy

If the grains on either side of the grain boundary are the same phase then the grain boundary energy can be expressed by

$$\sigma_{gb} = 2\sigma_{SL}\cos\theta, \tag{11}$$

where $\theta = \dfrac{\theta_A + \theta_B}{2}$ is the angle that the solid–liquid interfaces make with the y axis. The angles, θ_A and θ_B were obtained from the cusp coordinates (x, y) using a Taylor expansion for parts at the base of the groove. According to Eq.(11), the value of σ_{gb} should be smaller or equal to twice of solid–liquid interface energy, i.e. $\sigma_{gb} \leq 2\sigma_{SL}$.

The value of the grain boundary energy for the solid solution Ag_2Al (Ag_2Al–28.3at%$CuAl_2$) was found to be $(271.4\pm35.3)\times10^{-3}$J·m^{-2} using the values of the σ_{SL} and θ in Eq.(11). The estimated error in determination of θ angles was found to be 1%. Thus the total experimental error in the resulting grain boundary energy is about 13%.

A comparison of the values of the Gibbs–Thomson coefficient (Γ), solid–liquid interface energy ($\sigma_{SL)}$ and grain boundary energy ($\sigma_{gb)}$ for the solid solution Ag_2Al in the Al–Cu–Ag alloy obtained in the present work with the values of Γ, σ_{SL} and σ_{gb} for the same solid phase in the Al–Cu–Ag determined in a previous work is given in Table 4. As can be seen from Table 4, the value of ΔS_f for the solid solution Ag_2Al calculated in a previous work is four times smaller than the value of ΔS_f for the same solid phase calculated from the phase diagram as shown in Fig.1 in the present work. The resulting values of Γ, σ_{SL} and σ_{gb} for the solid solution Ag_2Al in the Al–Cu–Ag alloy disagree with the values of Γ, σ_{SL} and σ_{gb} obtained by Bulla *et al.*[36] The value of Γ for the solid solution Ag_2Al has been found to be in the range of $1.8\times10^{-8} - 3.7\times10^{-8}$K·m by Bulla *et al.*[36] The statistical fluctuation in their determination of Γ is about 95%.[36] As can be also seen from Table 4, the average value of Γ for the solid solution Ag_2Al obtained by Bulla *et al*[36] is about 50% smaller than the average value of Γ for the solid solution Ag_2Al obtained in the present work. Thus the value of σ_{SL} for the solid solution Ag_2Al obtained by Bulla *et al*[36] is not a reliable value and five times smaller than the value for the same solid phase obtained in the present work.

Table 4. A comparison of the values of Γ, σ_{SL} and σ_{gb} for the solid solution Ag_2Al in the Al–Cu–Ag alloy.

system	solid phase	liquid phase	temperature/K	entropy $\Delta S_f \times 10^6$/(J/K·m^3)	$\Gamma \times 10^{-8}$ /(K·m)	$\sigma_{SL} \times 10^{-3}$ /(J·m^{-2})	$\sigma_{gb} \times 10^{-3}$ /(J·m^{-2})
Al–Cu–Ag	Ag_2Al (Ag–38.60at%Ag–2.93at%Cu)[37]	Al–16.57at%Ag–11.87at%Cu[37]	775.09	1.17[36]	2.4 ± 0.6[36]	28± 7[36]	—
Al–Cu–Ag	Ag_2Al (Ag_2Al–28.3at%$CuAl_2$)[37]	$CuAl_2$–23.6at%Ag_2Al[37]	799.35	4.12[a]	3.5 ± 0.3[a]	145.9 ± 17.5[a]	271.4 ± 35.3[a]

[a] present work

The role of interfacial energy anisotropy is considered to play a critical role in many phase transformations. In the present work, the solid–liquid interfacial energy was assumed to be isotropic and the mean value of solid–liquid interfacial energy was obtained. In the literature, there are no theoretical and experimental available data for anisotropy of the interfacial

energy of the solid Ag_2Al phase.

4. Conclusions

A radial temperature gradient on the sample was established by heating from the centre with a single heating wire and cooling the outside of the sample with a heating/refrigerating circulating bath. The equilibrated grain boundary groove shapes for the solid solution Ag_2Al in the Al–Cu–Ag alloy system were observed from the quenched sample. The average values of the Gibbs–Thomson coefficient, solid–liquid interfacial energy and grain boundary energy for the solid solution Ag_2Al (Ag_2Al–28.3at%$CuAl_2$) in equilibrium with the eutectic liquid ($CuAl_2$–23.6at%Ag_2Al) have been determined from the equilibrated grain boundary groove shapes. The thermal conductivity of the solid phase for the Ag_2Al–28.3at%$CuAl_2$ alloy and the thermal conductivity ratio of the equilibrated liquid phase to solid phase at the melting temperature have also been measured with radial heat flow apparatus and Bridgman type growth apparatus.

Acknowledgements

The authors are grateful to the Scientific and Technical Research Council of Turkey (TÜBİTAK under Contact No 105T481) for their financial support.

References

[1] Eustathopoulos N, Nicholas M G and Drevet B 1999 *Wettability at HighTemperatures* Pergamon Materials Series (Oxford: Pergamon)
[2] Martin J W, Doherty R D and Cantor B 1997 *Stability of Microstructure in Metallic Systems* (Cambridg: Cambridge University Press)
[3] Turnbull D 1950 *J. Appl. Phys.* **2** 1022
[4] Jones D R H 1974 *J. Mater. Sci.* **9** 1
[5] Eustathopoulos N 1983 *Int. Met. Rev.* **28** 189
[6] Bolling G F and Tiller W A 1960 *J. Appl. Phys.* **31** 1345
[7] Jones D R H and Chadwick G A 1970 *Phil. Mag.* **22** 291
[8] Nash G E and Glicksman M E 1971 *Phil. Mag.* **24** 577
[9] Jones D R H and Chadwick G A 1971 *J. Cryst. Growth* **11** 260
[10] Jones D R H 1978 *Phil. Mag.* **27** 569
[11] Schaefer R J, Glicksman M E and Ayers J D 1975 *Phil. Mag.* **32** 725
[12] Hardy S C 1977 *Phil. Mag.* **35** 471
[13] Singh N B and Glicksman M E 1989 *J.Cryst. Growth* **98** 573
[14] Hoyt J J, Asta M, Haxhimali T, Karma A, Napolitano R E and Trivedi R 2004 *MRS Bulletin* **29** 935
[15] Gündüz M and Hunt J D 1985 *Acta Metall.* **33** 1651
[16] Gündüz M and Hunt J D 1989 *Acta Metall.* **37** 1839
[17] Maraşlı N and Hunt J D 1996 *Acta Matell.* **44** 1085
[18] Keşlioğlu K and Maraşlı N 2004 *Mater. Sci. and Eng.* A **369** 294
[19] Keşlioğlu K and Maraşlı N 2004 *Metall. Mater. Trans.* A **35A** 3665
[20] Erol M, Keşlioğlu K and Maraşlı N 2007 *J.Phys. Conden. Matter.* **19** 176003
[21] Erol M, Maraşlı N, Keşlioğlu K and Gündüz M 2004 *Scripta Mater.* **51** 131
[22] Maraşlı N, Akbulut S, Ocak Y, Keşlioğlu K, Böyük U, Kaya H and Çadırlı E 2007 *J. Phys. Condens Matter.* **19** 506102
[23] Akbulut S, Ocak Y, Maraşlı N, Keşlioğlu K, Böyük U, Çadırlı E and Kaya H 2008 *Mater. Charact.* **59** 1101
[24] Ocak Y, Akbulut S, Maraşlı N, Keşlioğlu K, Böyük U, Kaya H and Çadırlı E 2008 *Met. Mater. Int.* **14** 2
[25] Saatçi B, Çimen S, Pamuk H and Gündüz M 2007 *J. Phys. Conden. Matter* **19** 326219
[26] Meydaneri F, Saatçi B, Gündüz M and Özdemir M 2007 *Surf. Sci.* **601** 2171
[27] Keşlioğlu K, Gündüz M, Kaya H and Çadırlı E 2004 *Mater. Lett.* **58** 3067
[28] Bayender B, Maraşlı N, Çadırlı E, Şişman H and Gündüz M 1998 *J. Cryst. Growth* **194** 119
[29] Bayender B, Maraşlı N, Çadırlı E and Gündüz M 1999 *Mat. Sci. and Eng.* A **270** 343
[30] Maraşlı N, Keşlioğlu K and Arslan B 2003 *J. Cryst. Growth* **247** 613
[31] Ocak Y, Akbulut S, Böyük U, Erol M, Keşlioğlu K and Maraşlı N 2006 *Scr. Mater.* **55** 23
[32] Akbulut S, Ocak Y, Böyük U, Erol M, Keşlioğlu K and Maraşlı N 2007 *J. Appl. Phys.* **100** 123505
[33] Böyük U, Keslioğlu K and Maraşlı N 2007 *J. Phys. Condens. Matter* **19** 116202
[34] Ocak Y, Akbulut S, Keşlioğlu K and Maraşlı N 2008 *J. Colloid Interf. Sci.* **320** 555
[35] Ocak Y, Akbulut S, Keşlioğlu K and Maraşlı N 2008 *J. Phys.* D: *Appl. Phys.* **41** 065309
[36] Bulla A, Carreno-Bodensiek C, Pustal B, Berger R, Bührig-Polaczek A and Ludwig A 2007 *Metall. Mater. Trans.* A **38** 1956
[37] Witusiewicz V T, Hecht U, Fries S G and Rex S 2005 *J. Alloy Compd.* **387** 217
[38] Touloukian Y S, Powell R W, Ho C Y and Klemens P G 1970 *Thermal Conductivity Metallic Elements and Alloys* vol 1 (New York: Plenum) p60
[39] Touloukian Y S, Powell R W, Ho C Y and Klemens P G 1970 *Thermal Conductivity Metallic Elements and Alloys* vol 1 (New York: Plenum) p346
[40] Touloukian Y S, Powell R W, Ho C Y and Klemens P G 1970 *Thermal Conductivity Metallic Elements and Alloys* vol 1 (New York: Plenum) p81
[41] Christian J W 1975 *The Theory of Transformations in Metals and Alloys* Part I 2nd edn (Oxford: Pergamon)
[42] Tassa M and Hunt J D 1976 *J. Cryst. Growth* **34** 38
[43] Neumann J P 1966 *Acta Metall.* **14** 505